https://africanjournalofbiomedicalresearch.com/index.php/AJBR
Afr. J. Biomed. Res. Vol. 28(1s) (January 2025); 1128-1143
Research Article

Synthesis, Analgesic Evaluation, Molecular Docking and DFT Studies of Novel 4-Aminoantipyrine Derivatives

Al Luaibi Abeer Issa Mohammed[1,2], Munther Abduljaleel Muhammad-Ali[3], Md Azman Pkm Seeni Mohamed[1], Nozlena Abdul Samad[1], Nur Nadhirah Mohamad Zain[1], Mohd Yusmaidie Aziz[1]*

[1]*Department of Toxicology, Advanced Medical and Dental Institute, Universiti Sains Malaysia, Bertam, 13200, Kepala Batas, Penang, Malaysia
[2]Department of Pharmacy, Al-Manara College for Medical Sciences, Maysan 62001, Iraq
[3] Department of Ecology, College of Science, University of Basrah, Basrah 61001, Iraq

***Corresponding author:** Mohd Yusmaidie Aziz
*Email: mohd.yusmaidie@usm.my

Abstract
The present study investigates the analgesic efficacy of four newly synthesized 4-aminoantipyrine derivatives (4a-4d), which were obtained by conjugating 4-aminoantipyrine with oxadiazole and triazole moieties. The derivatives were evaluated for their analgesic properties using the writhing method in Swiss albino mice, revealing that compound 4c exhibited the highest activity (69%), comparable to paracetamol (71%). The remaining derivatives displayed varying degrees of analgesic activity. Molecular docking studies using MOE software demonstrated significant binding affinities of the derivatives to both mu-opioid (5C1M) and kappa-opioid (6B73) receptors, with compound 4c showing the strongest interactions. DFT calculations, performed with the Gaussian program, provided insights into the electronic structure and stability of the compounds, indicating their potential as effective analgesic agents. The study underscores the promise of these derivatives, particularly compound 4c, for further development in the field of analgesic drug discovery.

Keywords: 4-aminoantipyrine, Oxadiazole, Triazole, Analgesic activity, Molecular docking, DFT, Drug development

***Author for correspondence: Email:** *mohd.yusmaidie@usm.my*

Received: 12/01/2025 *Accepted: 18/01/2025*

DOI: https://doi.org/10.53555/AJBR.v28i1S.6363

Introduction

The quest for effective pain and inflammation management has traditionally relied on corticosteroids and non-steroidal anti-inflammatory drugs (NSAIDs), which, while effective, can lead to adverse effects with long-term use (Sohail et al., 2023). This has spurred the search for safer alternatives. Introduced in 1980, statins have emerged as a class of drugs not only effective in treating hyperlipidemia but also possessing anti-inflammatory and immunomodulatory properties that contribute to cardiovascular health (Blanco-Colio et al., 2003; Endo, 2010). Their ability to reduce inflammatory markers and modify immune cell activity has been well-documented, with clinical trials demonstrating their potential as analgesics (Proksch et al., 1990; Singh et al., 2009; Kitas et al., 2019).

The repurposing of drugs with known anti-inflammatory properties into analgesics represents a promising avenue in pharmaceutical research. Statins, for example, have been shown to exhibit analgesic effects in animal studies, suggesting their potential dual role in managing both inflammation and pain. Studies on animals have also shown that rosuvastatin has analgesic effects. Specifically, the study by Mohan et al. (2022) aimed to examine the interaction of rosuvastatin with other analgesics and to validate the analgesic properties of etoricoxib, tramadol, amlodipine, and amitriptyline. The findings revealed that rosuvastatin possesses dose-dependent analgesic activity that enhances the effects of the aforementioned analgesics.

Antipyrine, a compound with a pyrazolone moiety, was first synthesized in the late 18th century and became a widely used analgesic until the advent of aspirin. The chemical known as antipyrine, scientifically named 1,5-dimethyl-2-phenylpyrazole-3-one, features a pyrazolone moiety—a five-membered heterocyclic ring containing a ketone group and two adjacent nitrogen atoms (Sahoo et al., 2020). Ludwig Knorr coined the term "antipyrine" in the late 18th century to describe the first synthetic analgesic, which remained the most widely used pain medication until the synthesis of aspirin in the early 20th century (Adithya Krishnan et al., 2022). Through strategic derivatization, numerous antipyrine derivatives such as isopropyl antipyrine, aminopyrine, ramifenazone, and dipyrone have been developed and are now extensively used as analgesics and anti-inflammatory agents worldwide (Asif et al., 2021).

4-Aminoantipyrine (Ampyrone), distinguished by an amino group at the C-4 position, is notable for its broad spectrum of biological activities, as highlighted by Mohanram and Meshram (2014). This derivative of antipyrine serves as a versatile building block for the synthesis of a variety of compounds through a range of chemical reactions. For instance, amide compounds can be formed by reacting 4-aminoantipyrine with specific reagents such as chloroacetyl chloride, as detailed by Mishra et al. (2017). Furthermore, the fusion of 4-aminoantipyrine with other heterocyclic compounds can yield novel derivatives with augmented biological activity, as reported by Alkhzem et al. (2022).

The anti-inflammatory and analgesic properties of 4-aminoantipyrine (4-amino-1,5-dimethyl-2-phenylpyrazole-3-one) and its analogues have been recognized as substances of significant interest, as reported by Alam et al. (2012). Fadda and Elattar (2015) conducted a synthesis and evaluation of several enaminonitrile derivatives of antipyrine, which were considered as potential novel agents for anti-inflammatory and analgesic applications. These researchers produced various aldehydes of 4-aminophenazone Schiff base derivatives. The synthesized compounds were then tested for their ability to mitigate inflammation, alleviate pain, and reduce fever. The results indicated that these substances indeed possess analgesic properties, as evidenced by a significant decrease in paw-licking and writhing behavior in treated mice, as detailed by Murtaza et al. (2017).

This study investigates the synthesis of four novel derivatives of 4-aminoantipyrine, with the aim of evaluating their analgesic properties. By leveraging the established pharmacological profile of 4-aminoantipyrine, this study seeks to contribute to the development of new analgesics that could offer improved safety and efficacy profiles. The findings from this study could pave the way for new therapeutic strategies in pain management.

Materials and Methods

Chemicals and Materials

4-aminoantipyrine from Sigma Aldrich (AL-Qiffaf Scientific Co., Baghdad, Iraq), phenyl *iso*-thiocyanate from Thomas Baker (Mumbai, India), carbon disulfide from ALPHA Chemika Co., (Mumbai, India), Chloroacetyl chloride, 3-Chloropropionyl chloride and thiophene-2-carbohydrazide from Suzhou Leah Chemical company (Hefei, China), sodium hydroxide and sodium acetate from Merck (AL-Qiffaf Scientific Co., Baghdad, Iraq), and dioxane, ethanol, and chloroform from Fluka (Baghdad, Iraq) were utilized in the study.

Synthesis of compounds

The compounds N-(1,5-dimethyl-3-oxo-2-phenyl-2,3-dihydro-1H-pyrazol-4-yl)-2-((5-(thiophen-2-yl)-1,3,4-oxadiazol-2-yl)thio) acetamide (***4a***), N-(1,5-dimethyl-3-oxo-2-phenyl 2,3-dihydro-1H-pyrazol-4-yl)-2-((4-phenyl-5-(thiophen-2-yl)-4H-1,2,4-triazol-3-yl)thio) acetamide (***4b***), N-(1,5-dimethyl-3-oxo-2-phenyl-2,3-dihydro-1H-pyrazol-4-yl)-3-((5-(thiophen-2-yl)-1,3,4-oxadiazol-2-yl)thio)propenamide (***4c***) and N-(1,5-dimethyl-3-oxo-2-phenyl-2,3-dihydro-1H pyrazol-4-yl)-3-((4-phenyl-5-(thiophen-2-yl)-4H-1,2,4-triazol-3-yl)thio)propenamide (***4d***) were synthesized and characterized according to Mohammad et al., (2021), as shown in Scheme 1-4.

Evaluation of analgesic activity by writhing test

There were six groups of albino mice (n= 36), with six animals (three female and three male) in each group. All mice had fasted overnight. Group 1, mice received 10 mL/kg of vehicle (olive oil) as a control group; Group 2, mice received 10 mg/kg of paracetamol as a standard group; and Groups 3–6, mice received 10 mg/kg of drugs under investigation (4a, 4b, 4c or 4d) orally. Using gastric gavage, each dosage of the chemicals, paracetamol, and experimental medications was given orally. Mice in each group were given 10 mL/kg of a 1% v/v acetic acid solution intraperitoneally (i.p.) after an hour (pain) in order to create the nociception condition. Starting five minutes after the acetic acid was administered, the number of writhing that were seen in each mouse was counted for fifteen minutes (Yimer et al., 2020, Ezeja et al., 2011).

To determine the analgesic potency, the percentage inhibition (I%) of writhing (abdominal constrictions) was calculated using Equation 1.

$$Inhibition\%\ (I\%) = \left(\frac{N_c - N_t}{N_c}\right) x100 \qquad (1)$$

In the control group, N_c represents the average of the writhing numbers (group 1), while N_t represents the average of the writhing numbers in the testing groups (Ganeshpurkar and Rai, 2013). The animal study has been approved by Ethical Committee for Human and Animal Model Research – College of Pharmacy, University of Basrah.

Molecular docking studies

Molecular docking of the synthesized series of compounds was performed using MOE 2015 v10 Molecular Operating Environment (St John's Innovation Centre, Cowley Road, Cambridge, CB4 0WS, UK) and all water and ligand molecules were removed. Crystal structure of active mu-opioid receptor bound to the agonist BU72 (protein ID: 5C1M) and Crystal Structure of a nanobody-stabilized active state of the kappa-opioid receptor (proteins ID: 6B73) were obtained from RCSB protein data bank.

Density Functional Theory (DFT) study

The DFT calculation was carried out in the ground state with Gaussian 09 software by using B3LYP/6–31 G* method. The geometrical, electronic and energy parameters were extracted from the Gaussian files based on the optimized structures.

Results and Discussion

The final compounds ***4a***, ***4b***, ***4c*** and ***4d*** were synthesized by nucleophilic substitution of ionized sulfur (-S^-) atom of oxadiazole or triazole thiols attacked to methylene group (-CH_2-Cl) of **4**-aminoantipyrine derivatives, the byproducts acetic acid and sodium chloride were formed. The mechanism of the reaction occurred according to S_N2 (Wang et al., 2016). Schemes 1-4 represent the chemical routes used to synthesis of compounds ***4a***, ***4b***, ***4c***, and ***4d***

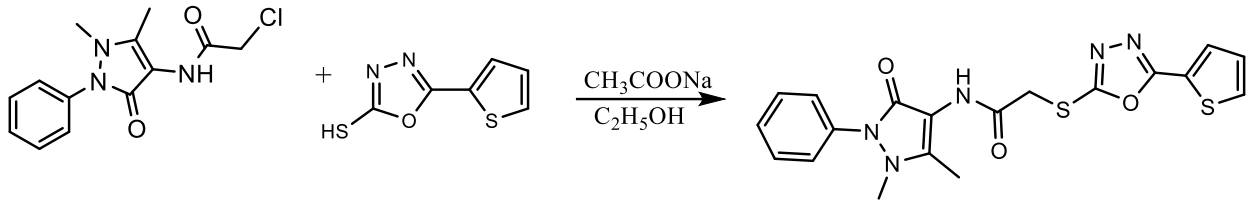

Scheme 1. Synthesis of *4a* (N-(1,5-dimethyl-3-oxo-2-phenyl-2,3-dihydro-1H-pyrazol-4-yl)-2-((5-(thiophen-2-yl)-1,3,4-oxadiazol-2-yl) thio) acetamide)

4a: White crystals, 74% yield, m. p. 218-219ºC, IR (KBr): ν (cm^{-1}) = 3174 (N-H), 3117 (C-H, aromatic), 2989, 2847 (C-H, aliphatic), 1685, 1643 (C=O, amide), 1589 (C=N), 1535, 1477 (C=C), 1323, 1172 (C-O, C-N). ^{1}H NMR (DMSO-d_6): δ (ppm) = 9.51 (s, 1H, NH), 7.95 (dd, 1H, thiophene-Hc), 7.83 (dd, 1H, thiophene-Ha), 7.29 (m, 1H, thiophene-Hb), 7.53-7.49 (m, 2H, *J* = 7.51 Hz, Ar-H_{meta}), 7.36-7.28 (m, 3H, *J* = 7.35 Hz, Ar-$H_{ortho, para}$), 4.29 (s, 2H, -CH_2-), 3.05 (s, 3H, N-CH_3), 2.11 (s, 3H, C-CH_3). Analysis: calcd (found) for $C_{19}H_{17}N_5O_3S_2$ (427.50): C, 53.38 (53.49), H, 4.01 (3.96), N, 16.38 (15.95).

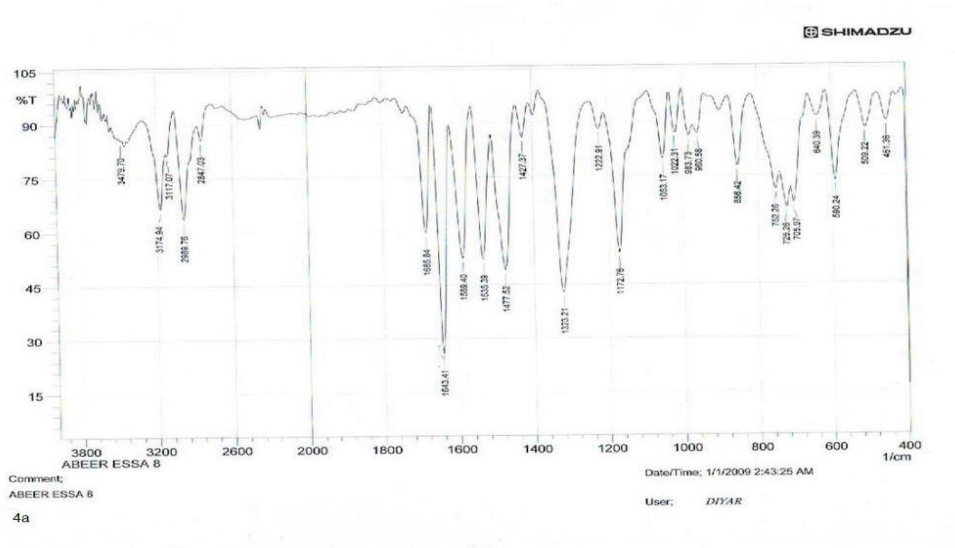

Figure 1. IR spectrum of compound 4a

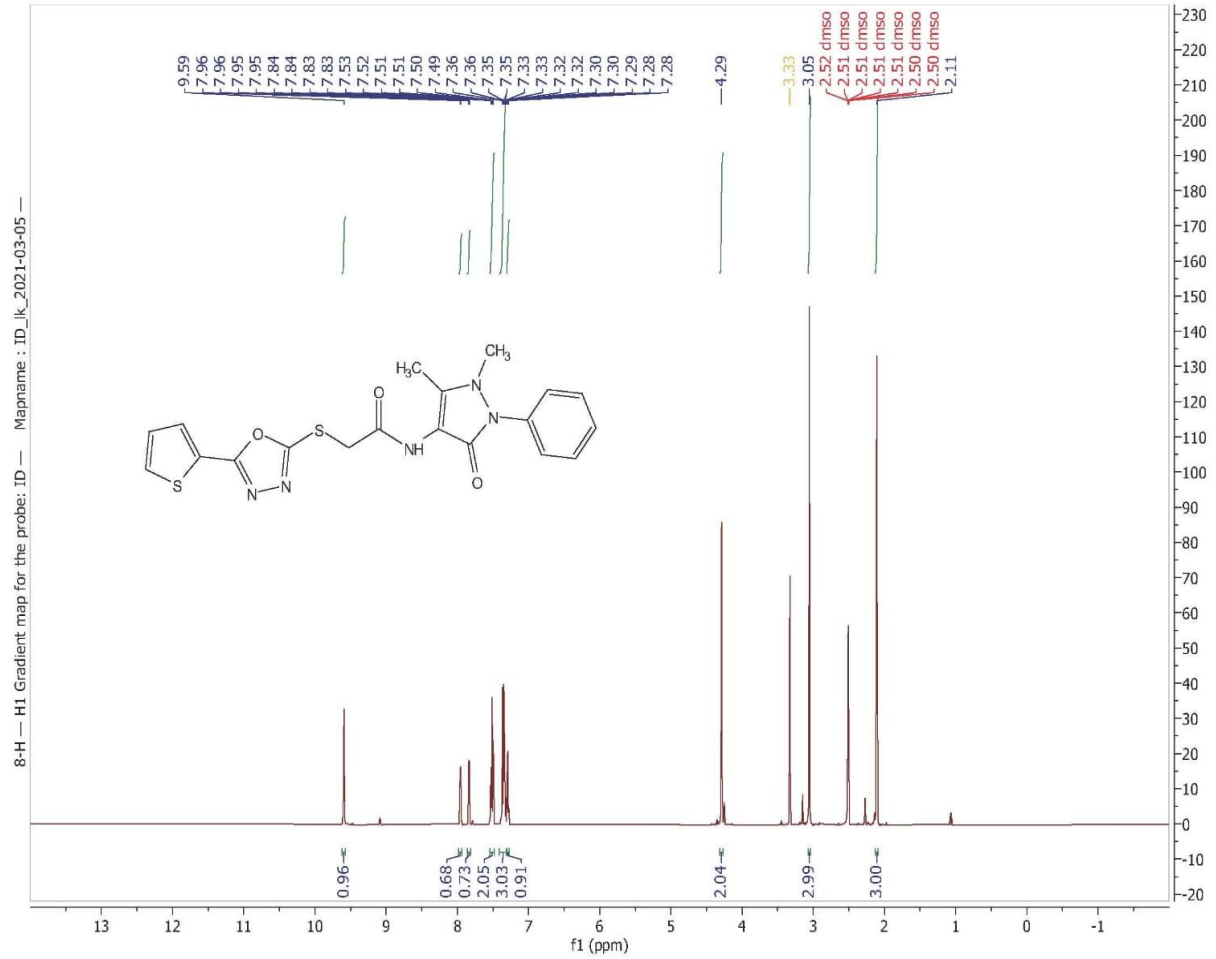

Figure 2. ^{1}HNMR-spectrum of compound 4a

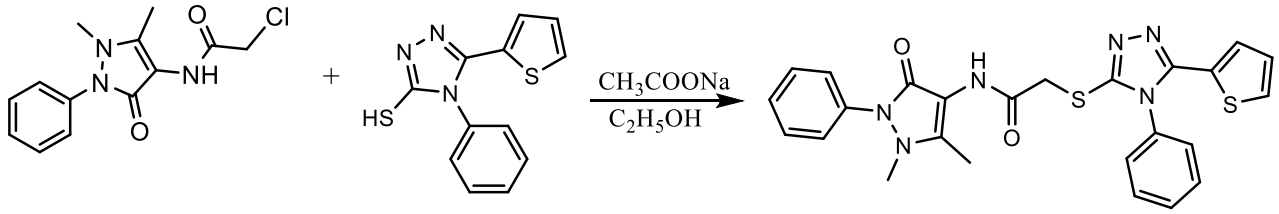

Scheme 2. Synthesis of *4b* (N-(1,5-dimethyl-3-oxo-2-phenyl-2,3-dihydro-1H-pyrazol-4-yl)-2-((4-phenyl-5-(thiophen-2-yl)-4H-1,2,4-triazol-3-yl) thio) acetamide)

4b: White crystal, 66% yield, m. p. 220-222ºC, IR (KBr): ν (cm^{-1}) = 3178 (N-H), 3043 (C-H, aromatic), 2928 (C-H, aliphatic), 1678, 1639 (C=O, amide), 1581 (C=N), 1538, 1492 (C=C), 1311, 1192 (C-N). ^{1}H NMR (DMSO-d_6): δ (ppm) = 9.52 (s, 1H, NH), 7.68-7.55 (m, 5H, Ar-H triazole attach and 1H, thiophene-Hc), 6.72 (dd, 1H, thiophene-Ha), 7.00 (m, 1H, thiophene-Hb), 7.52-7.31 (m, 5H, Ar-H pyrazole attach), 4.11 (s, 2H, -CH_2-), 3.05 (s, 3H, N-CH_3), 2.12 (s, 3H, C-CH_3). Analysis: calcd (found) for $C_{25}H_{22}N_6O_2S_2$ (502.61): C, 59.74 (58.78), H, 4.41 (4.24), N, 16.72 (16.45).

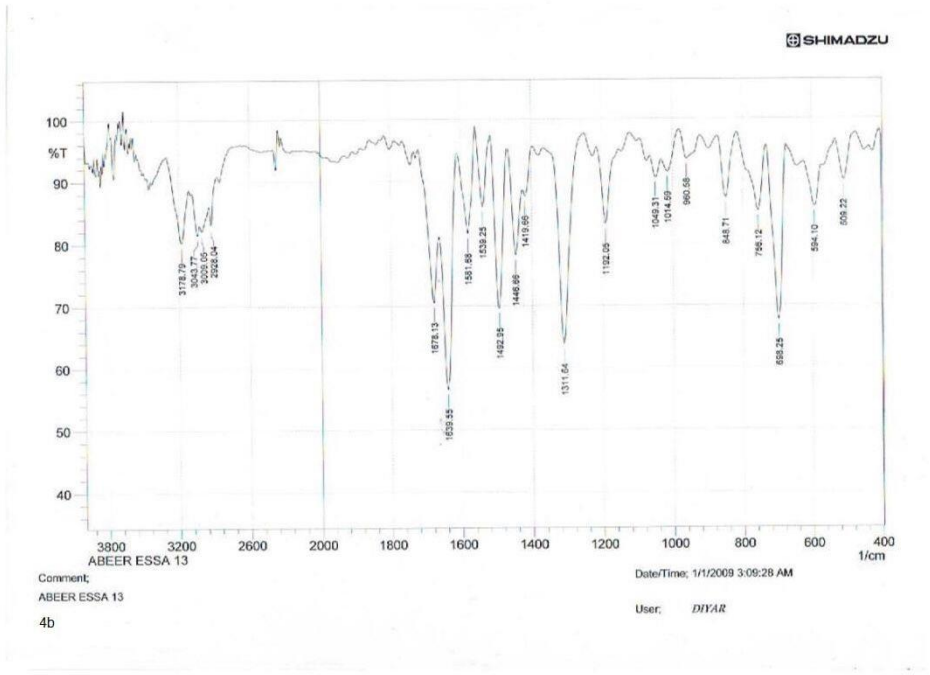

Figure 3. IR spectrum of compound 4b

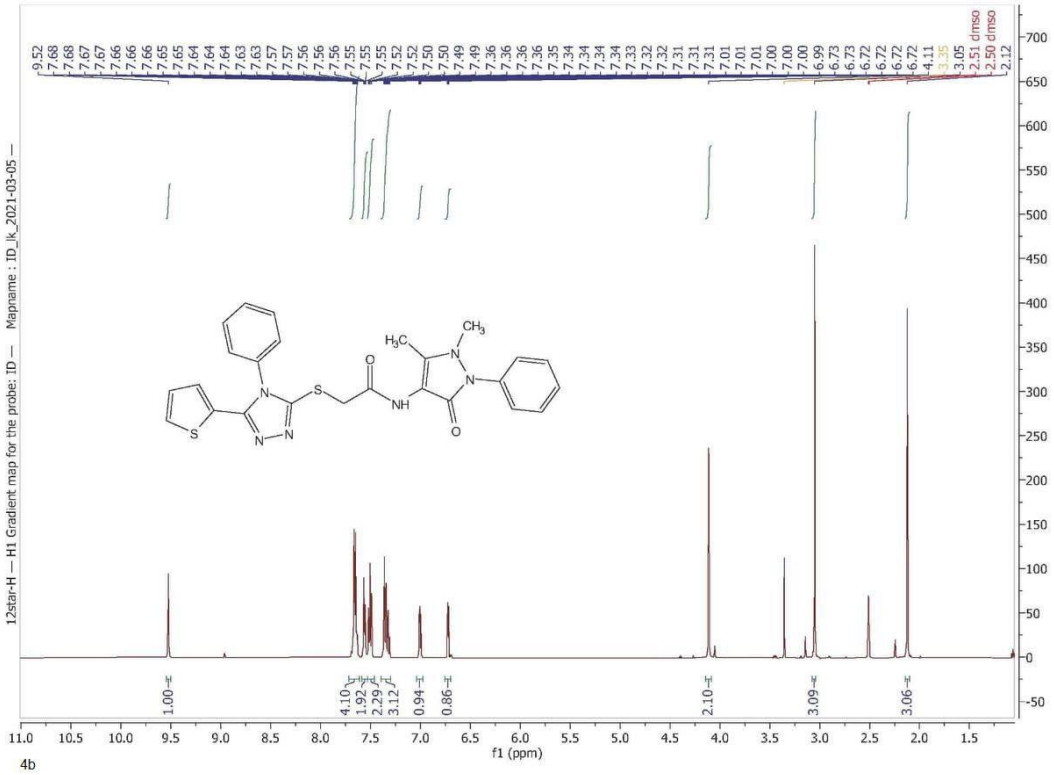

Figure 4. 1HNMR-spectrum of compound 4b

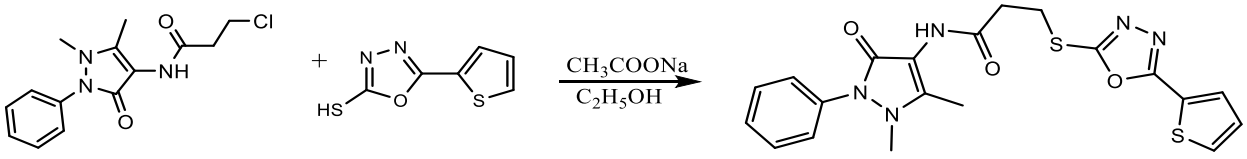

Scheme 3. Synthesis of *4c* (N-(1,5-dimethyl-3-oxo-2-phenyl-2,3-dihydro-1H-pyrazol-4-yl)-3-((5-(thiophen-2-yl)-1,3,4-oxadiazol-2-yl) thio) propenamide)

4c: White crystals, 78% yield, m. p. 193-195ºC, IR (KBr): ν (cm^{-1}) = 3178 (N-H), 3036 (C-H, aromatic), 2924 (C-H, aliphatic), 1681, 1647 (C=O, amide), 1589 (C=N), 1543, 1473 (C=C), 1303, 1238, 1176 (C-O, C-N). ^{1}H NMR (DMSO-d_6): δ (ppm) = 9.27 (s, 1H, NH), 7.955 (dd, 1H, sthiophene-Hc), 7.83 (dd, 1H, thiophene-Ha), 7.29 (m, 1H, thiophene-Hb), 7.52-7.32 (m, 5H, Ar-H pyrazole attach), 3.52 (t, 2H, *J* = 6.7 Hz, -CH_2-S-), 2.89 (t, 2H, *J* = 6.7 Hz, -CH_2-), 3.05 (s, 3H, N-CH_3), 2.13 (s, 3H, C-CH_3). Analysis: calcd (found) for $C_{20}H_{19}N_5O_3S_2$ (441.52): C, 54.41 (54.00), H, 4.34 (4.24), N, 15.86 (15.57).

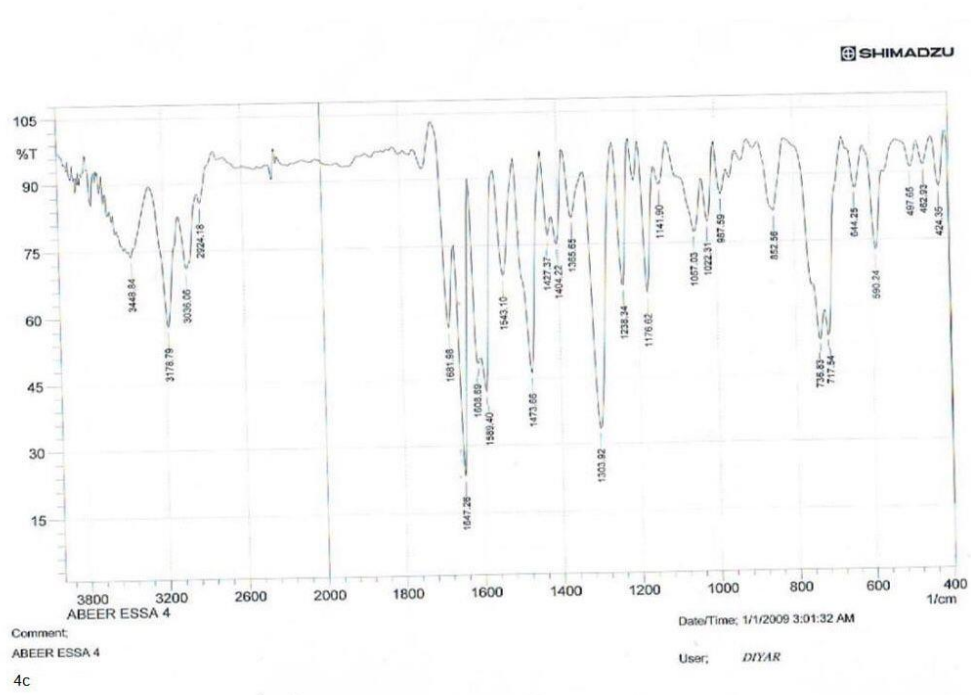

Figure 5. IR spectrum of compound 4c

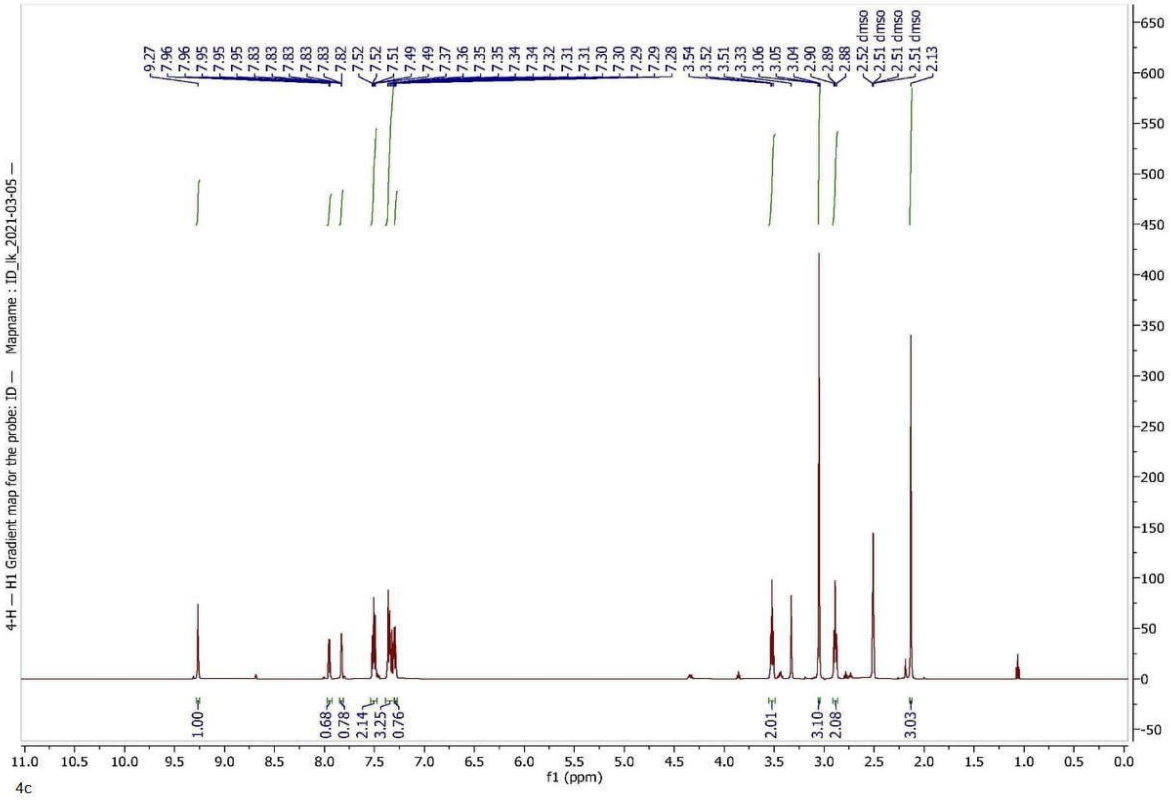

Figure 6. 1HNMR-spectrum of compound 4c

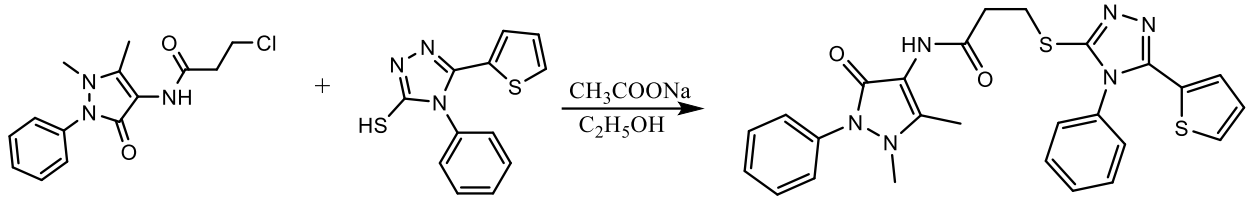

Scheme 4. Synthesis of *4d* (N-(1,5-dimethyl-3-oxo-2-phenyl-2,3-dihydro-1H-pyrazol-4-yl)-3-((4-phenyl-5-(thiophen-2-yl)-4H-1,2,4-triazol-3-yl) thio) propenamide)

4d: White crystals, 78% yield, m. p. 202-204ºC, IR (KBr): ν (cm^{-1}) = 3155 (N-H), 3055 (C-H, aromatic), 2916 (C-H, aliphatic), 1674, 1647 (C=O, amide), 1581 (C=N), 1496, 1435 (C=C), 1315, 1236 (C-N). Analysis: calcd (found) for $C_{26}H_{24}N_6O_2S_2$ (516.64): C, 60.45 (60.05), H, 4.68 (4.46), N, 16.27 (16.14).

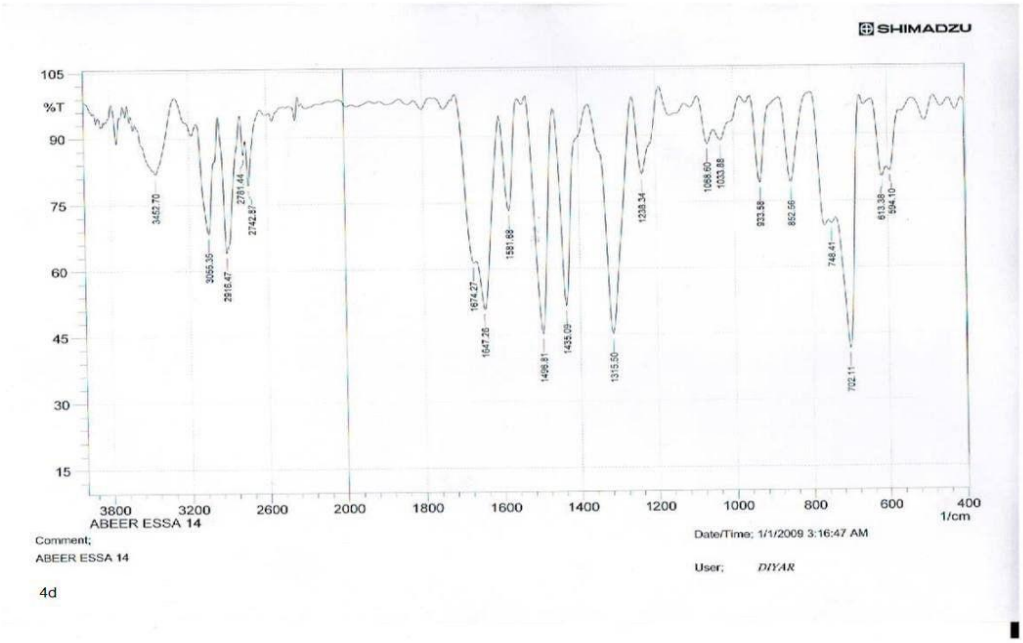

Figure 7. IR spectrum of compound 4d

The synthesis of compounds ***4a, 4b, 4c,*** and ***4d*** involves specific thiols and variations in the substitution position on the methylene group. Compound ***4a*** is synthesized by reacting a 1,3,4-oxadiazole thiol with a 4-aminoantipyrine derivative, resulting in an acetamide linkage. In contrast, compound ***4b*** uses a thiol derived from a 1,2,4-triazole compound with a phenyl group, also forming an acetamide linkage. Compound ***4c***, however, involves a different substitution position on the methylene group when reacting the 1,3,4-oxadiazole thiol with the 4-aminoantipyrine derivative, leading to a propenamide linkage. Similarly, compound ***4d*** is synthesized using a triazole thiol with a different substitution pattern, resulting in a structural isomer with a propenamide linkage. Although the nucleophilic substitution reaction mechanism remains consistent, the variations in thiol types and substitution positions yield distinct chemical structures, potentially leading to different biological activities.

Analgesic Activity

In Figure 1, it is evident that compound ***4c*** exhibited the highest activity (69%) among all tested compounds. Conversely, compounds ***4a*** and ***4d*** displayed moderate activity (24% and 30% respectively), while compound ***4b*** demonstrated weak activity (10%) compared to the standard drug. The notable activity of compound 4c can be attributed to its chemical structure and the impact of thioether crosslinks, which are commonly employed as spacers. Furthermore, the presence of heterocyclic rings, particularly oxadiazole, in these compounds contributed to their enhanced activity. The inclusion of these heterocyclic rings influences the physicochemical and pharmacokinetic properties of the entire compound (Rusu et al., 2023; Meanwell, 2023), as depicted in Figure 8.

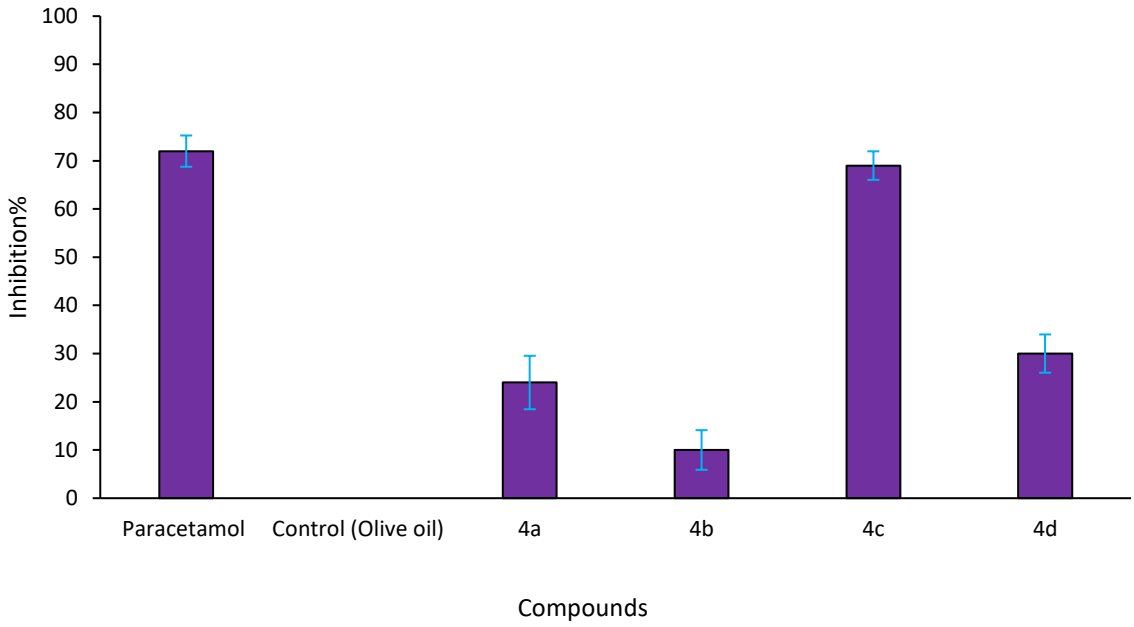

Figure 8. Analgesic activity inhibition percentage (%) by the writhing test of 4-aminoantipyrine derivatives

Molecular docking studies

The outcomes presented in Tables 1 and 2 feature the anticipated docking scores. Each of the synthesized compounds underwent covalent docking within the principal pocket of the active mu-opioid receptor, engaged with the agonist BU72 (5C1M), and the kappa-opioid receptor (6B73) in its nanobody-stabilized active configuration.

Table 1. Molecular docking score, RMSD, and binding affinity of the 4-aminoantipyrine derivatives

Comp.	**S Score kcal/mol**	**RMSD Å**	**Bonds between Atoms of Compounds and Residues of Active Site of 5C1M protein**						
			Comp. Atoms	Receptor Atoms	Receptor Residues	Interaction	d (Å)	E (kcal/mol)	Total E (kcal/mol)
4a	-8.37	1.85	N6 S8	OD2 OD2	ASP147 ASP147	H-donor H-donor	2.88 3.68	-8.2 -1.3	-44.79
4b	-9.97	1.67	5-ring 6-ring	CA 6-ring	SER55 TYR326	pi-H pi-pi	3.95 3.81	-0.6 -0.0	-44.73
4c	-8.41	1.92	S11	NE1	TRP318	H-acceptor	3.74	-0.8	-50.25
4d	-9.52	1.58	N9 S11 S24	OD2 SD O	ASP147 MET151 HIS54	H-donor H-donor H-donor	2.92 3.49 3.80	-7.3 -0.1 -0.6	-54.41
Paracetamol	-4.75	1.89	6-ring	CA	SER55	pi-H	3.74	-0.6	-19.46

Table 2. Molecular docking score, RMSD, and binding affinity of 4-aminoantipyrine derivatives

Comp.	**S Score kcal/mol**	**RMSD Å**	**Bonds between Atoms of Compounds and Residues of Active Site of 6B73 protein**						
			Comp. Atoms	Receptor Atoms	Receptor Residues	Interaction	d (Å)	E (kcal/mol)	Total E (kcal/mol)
4a	-8.04	1.48	N6 O38	OD2 OH	ASP138 TYR312	H-donor H-acceptor	3.11 3.26	-7.1 -1.3	-44.17
4b	-8.51	1.88	N6	OD2	ASP138	H-donor	2.96	-2.7	-45.48
4c	-7.98	1.52	S24 5-ring	O CG2	ASP138 ILE294	H-donor pi-H	3.50 4.07	-0.8 -1.0	-33.15
4d	-9.34	2.02	N9	OD2	ASP138	H-donor	3.05	-1.5	-42.18
Paracetamol	-4.73	1.49	N3	SD	MET142	H-donor	4.32	-1.6	-20.58

Tables 2 and 3 present the outcomes regarding the stability of ligands (synthesized compounds) with two proteins. The total energy ranged from -44.73 to -54.41 kcal/mol with protein 5C1M, and from -33.15 to -45.48 kcal/mol with protein 6B73, both yielding negative values. Examining the interaction sites, ligand 4d

engaged nitrogen and sulfur atoms, forming three hydrogen bonds with amino acids ASP147, MET151, and HIS54 within the largest pocket of protein 5C1M, at a distance of 1.58 Å. Conversely, the same ligand 4d interacted with protein 6B73 via a hydrogen bond between the nitrogen atom of the amide spacer and amino acid ASP138, with a distance of 2.02 Å, as depicted in Figures 9 and 10.

Compared to paracetamol, which falls within a range of -4.75 to -4.73 kcal/mol, the synthesized compounds displayed favorable docking scores ranging from -8.37 to -9.97 kcal/mol with the 5C1M protein, and they exhibited affinities ranging from -7.98 to -9.34 kcal/mol with the 6B73 protein. Each synthetic chemical demonstrated an RMSD value between 1.48 and 2.02. The simulation depicted in Figures 9 and 10 revealed that the synthesized chemical, interacting with mu-opioid and kappa-opioid receptors, respectively, exhibited superior accuracy compared to conventional medications targeting these receptors.

The molecular docking analysis of compounds within the binding sites of proteins 5C1M and 6B73 revealed that compounds 4b and 4d exhibited the highest docking scores of -9.97 and -9.52 kcal/mol, respectively, for 5C1M, and -8.51 and -9.84 kcal/mol, respectively, for 6B73. In comparison, compounds 4a and 4c showed lower binding energies of -8.37 and -8.41 kcal/mol, respectively, with 5C1M, and -8.04 and -7.98 kcal/mol, respectively, with 6B73. This difference may be attributed to the compounds' ability to tightly bind to the closed binding sites by increasing the spacer length from a methylene to an ethylene group (Bachurin et al., 2021).

Moreover, concerning analgesic activity, compound 4c exhibited potent activity compared to the standard drug paracetamol (with S Scores of "-4.75 and "-4.73 kcal/mol for 5C1M and 6B73 protein, respectively), possibly due to the enhancement of heterocyclic groups in this activity (Shyma et al., 2013)

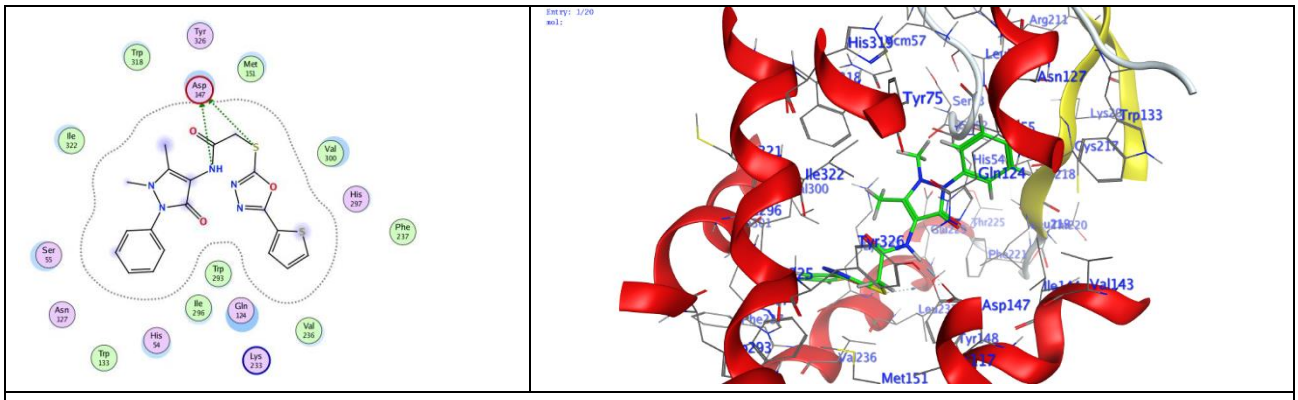

4a

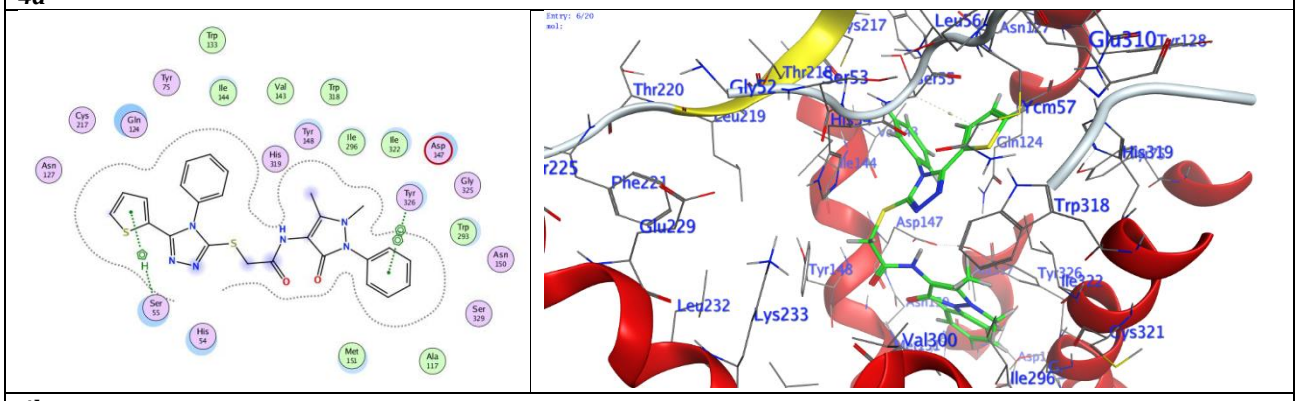

4b

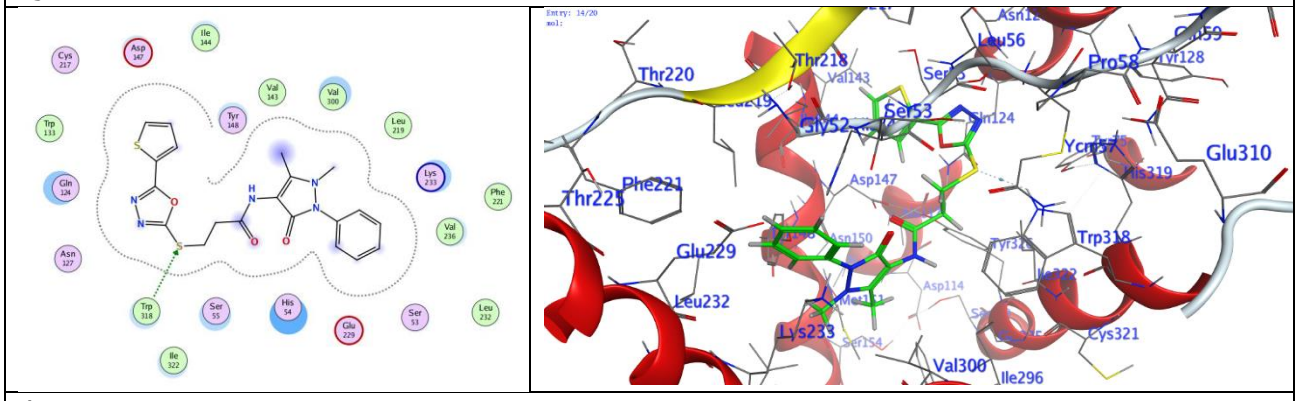

4c

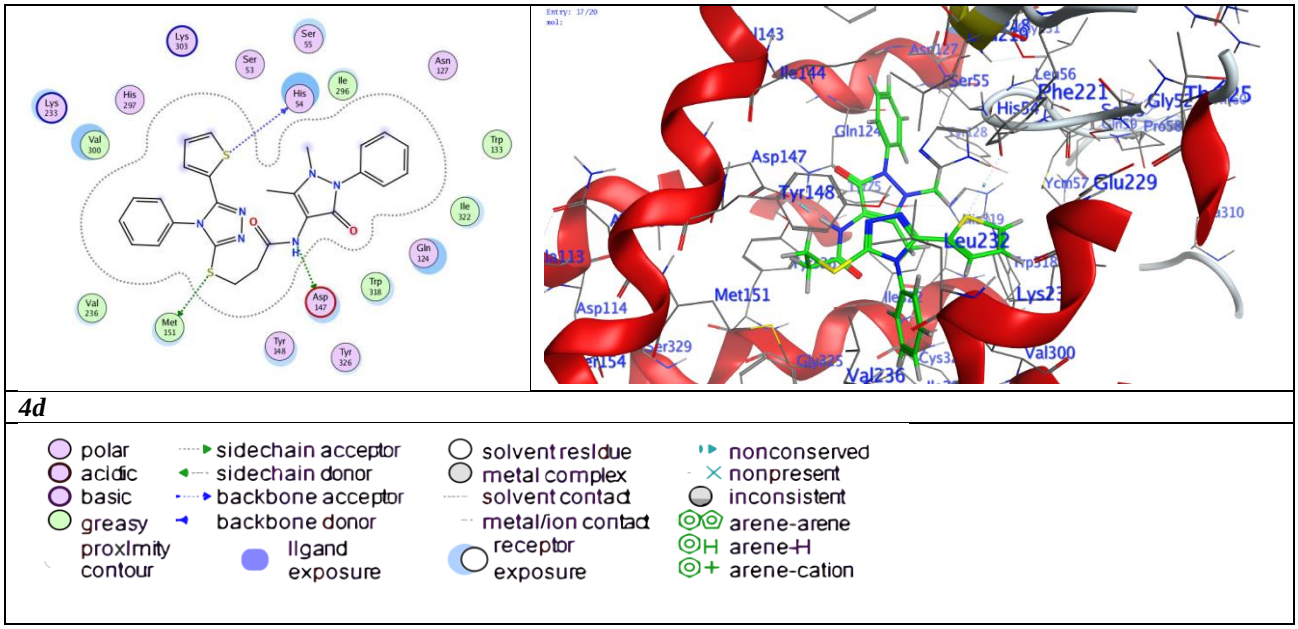

4d

Figure 9. The 2D and 3D binding affinity of the compounds with 5C1M

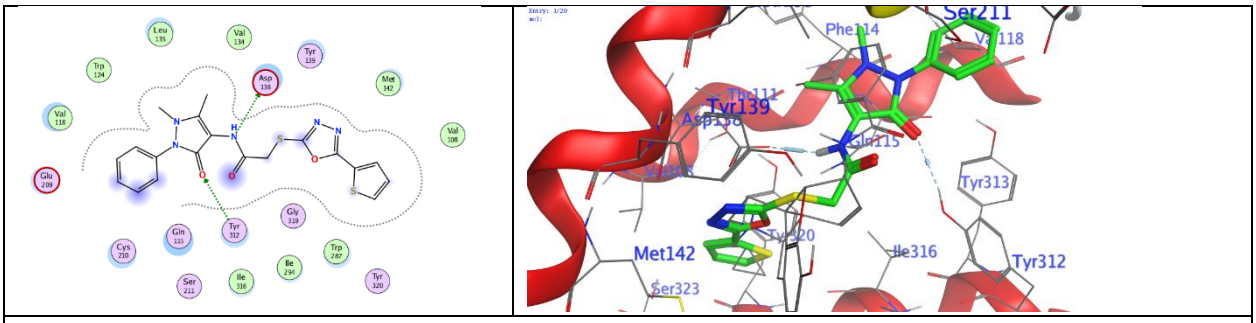

4a

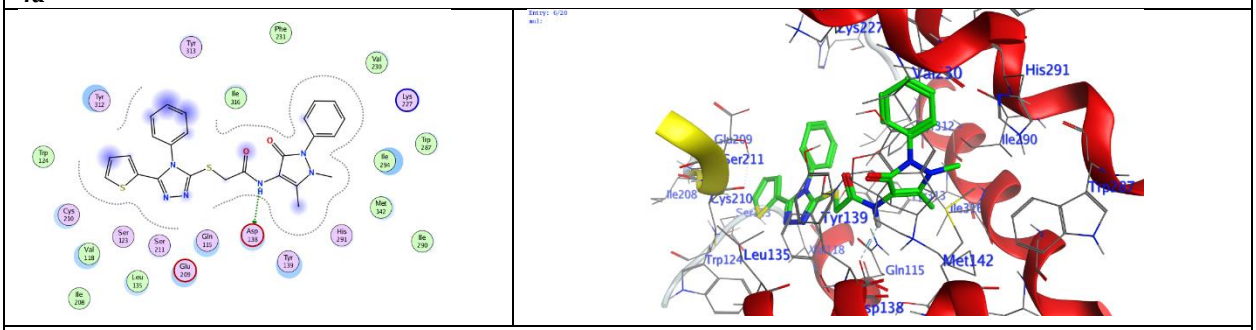

4b

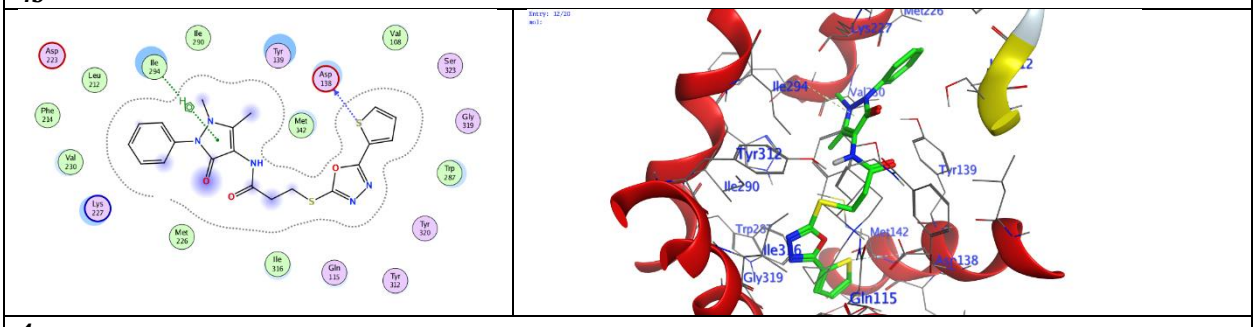

4c

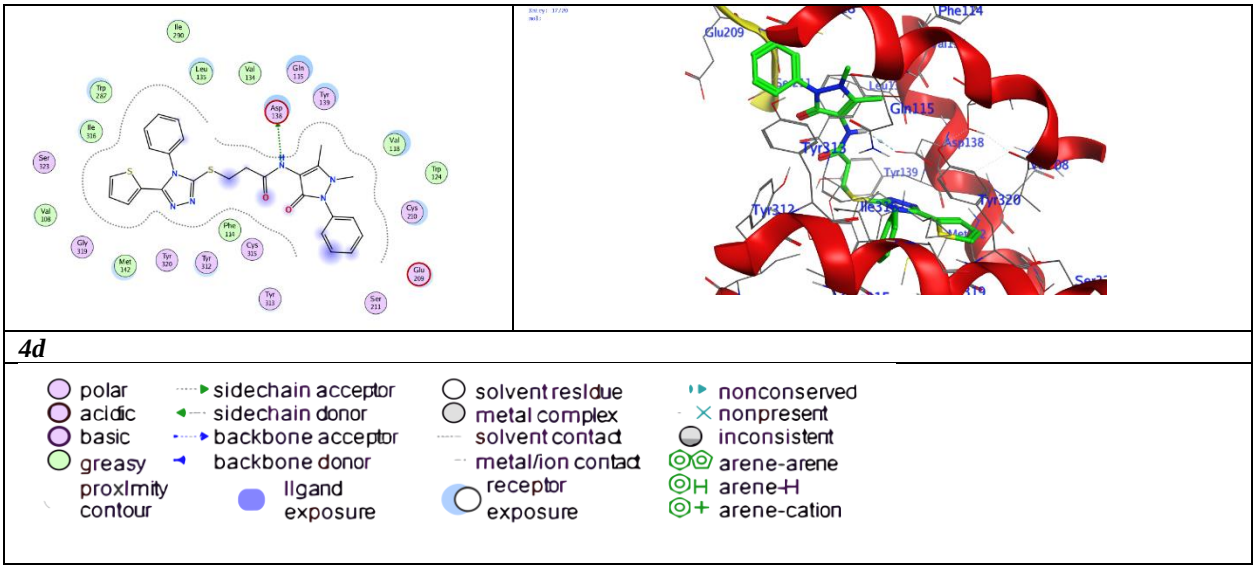

Figure 10. The 2D and 3D binding affinity of the compounds with 6B73

Density functional theory (DFT) Studies

Optimization of molecular geometries

The compounds depicted in Figure 11 have undergone optimization to explore their theoretical properties using Gaussian 09 software.

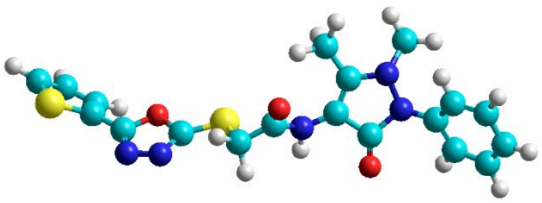

4a: N-(1,5-dimethyl-3-oxo-2-phenyl-2,3-dihydro-1H-pyrazol-4-yl)-2- ((5-(thiophen-2-yl)-1,3,4-oxadiazol-2-yl)thio) acetamide

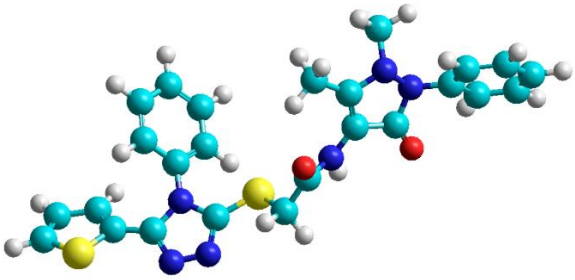

4b: N-(1,5-dimethyl-3-oxo-2-phenyl2,3-dihydro-1H-pyrazol-4-yl)-2-((4-phenyl5-(thiophen-2-yl)-4H-1,2,4-triazol-3-yl)thio) acetamide

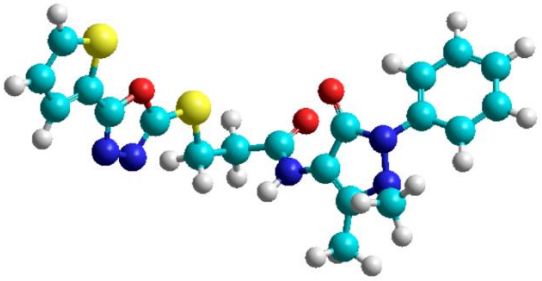

4c: N-(1,5-dimethyl-3-oxo-2-phenyl2,3-dihydro-1H-pyrazol-4-yl)-3-((5-(thiophen-2- yl)-1,3,4-oxadiazol-2-yl)thio)propanamide

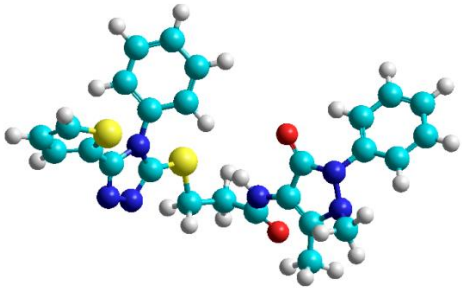

4d: N-(1,5-dimethyl-3-oxo-2-phenyl-2,3-dihydro-1H-pyrazol-4-yl)-3-((4-phenyl-5-(thiophen-2-yl)-4H-1,2,4-triazol-3-yl)thio)propanamide

Figure 11. IUPAC nomenclature and three-dimensional configurations

Lipophilicity

One important physicochemical property essential for drug development and discovery is lipophilicity. It significantly influences various phases of a drug's action, including pharmacokinetics, pharmacodynamics, and pharmacological effects (Glassman and Muzykantov, 2019). Log P serves as a predictive measure for assessing how effectively drugs will be absorbed through the intestinal epithelium, as it correlates with a compound's lipophilicity. In Table 3,

lipophilicity values for all synthesized compounds were documented, ranging from 2.45 to 4.57. Considering the common observation that orally absorbed compounds typically exhibit a logarithm of the partition coefficient (log P) lower than 5, a promising drug candidate should ideally possess a log P value below this threshold (Chandrashekar and Rani, 2008).

Table 3. Calculated molecular properties of 4-aminoantipyrine derivatives

Comp.	MW	Volume (Å3) /Area (Å2)	Charge O atom	μ (*Debye*)	logP
4a	427.50	1137.37/578.33	[O(7) -0.313] [O(15) -0.206] [O(29) -0.203]	4.326	2.45
4b	502.61	1336.40/632.57	[O(15) -0.332] [O(29) -0.316]	7.134	4.52
4c	441.52	1183.43/593.88	[O(38) -0.112] [O(3) -0.317] [O(17) -0.270]	3.500	2.46
4d	516.64	1368.62/636.37	[O(4) -0.347] [O(18) -0.313]	3.845	4.57

Mulliken atomic charges

Table 4 and Figure 12 present the Mulliken atomic charges for the compounds determined through the B3LYP/6–31 G* method. In the distribution of Mulliken charges, the oxygen atom of the amide carbonyl group of spacers ranged from -0.206 to -0.347, while that of the carbonyl atom of cyclic amide ranged from -0.203 to -0.316. Conversely, the oxygen atoms of the pyrrole ring exhibited values of -0.313 and -0.112 for 4a and 4c, respectively. Moreover, it has been observed that specific nitrogen atoms in the amide group of the spacers also displayed negative values ranging from -0.267 to -0.304.

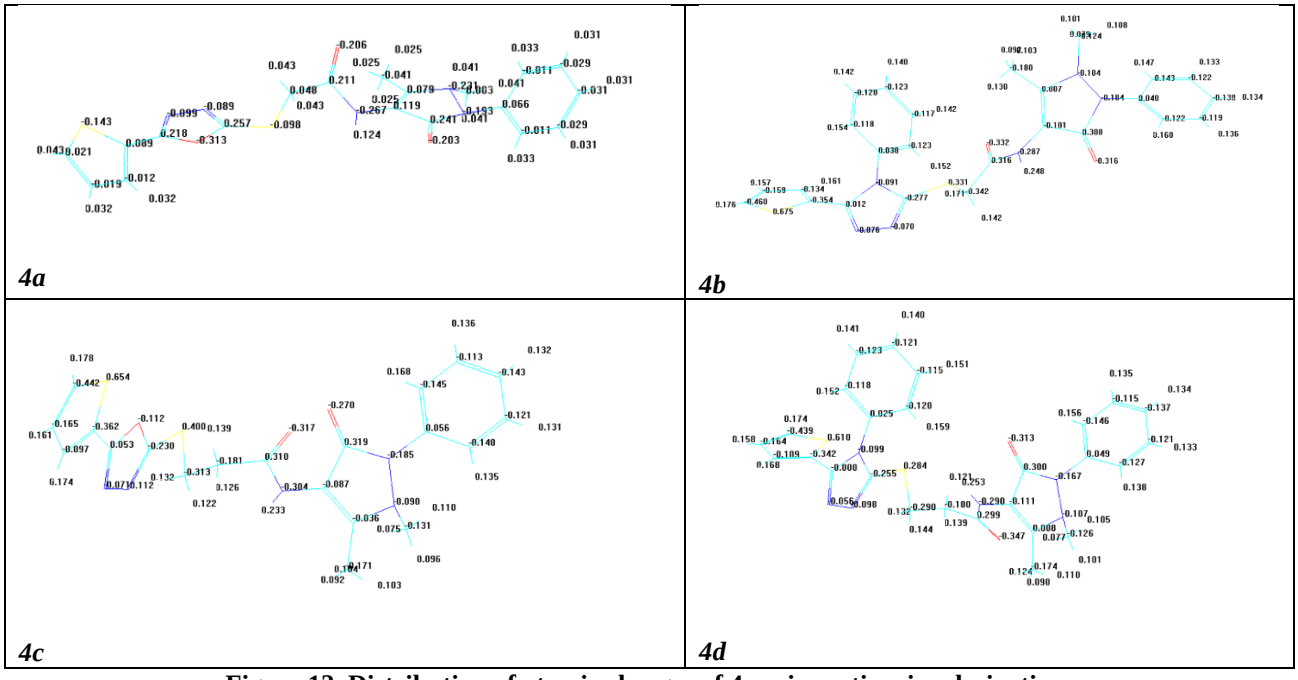

Figure 12. Distribution of atomic charges of 4-aminoantipyrine derivatives

Electric dipole moments

The dipole moment, a characteristic of polar molecules, refers to the distribution of electric charge and is associated with the electric field. One aspect of a particular molecule that remains unaffected by its surroundings is its polarity. The dipole moment is primarily determined by the distance between the charge separation and the variance in electronegativity. Table 4 illustrates the dipole moment values for the compounds (ranging from 3.500 to 7.134D). The ranking of dipole moments for compound 4b (7.134 D) is higher than that of 4a (4.326 D), followed by 4d (3.845 D), and then 4c (3.500 D).

Global reactivity descriptors

Frontier molecular orbitals (FMOs), comprising the Highest Occupied Molecular Orbital (HOMO) and Lowest Unoccupied Molecular Orbital (LUMO), play pivotal roles in evaluating molecular chemical stability, reactivity, and hardness/softness (Yu et al., 2022). In quantum chemical computations, accurately determining the energies associated with the HOMO (acting as a π donor) and LUMO (acting as a π acceptor) is essential. These orbitals primarily serve as electron donors (HOMOs) or electron acceptors (LUMOs). The molecular orbitals known as frontier molecular orbitals (FMOs) can also be referred to by another name. As

illustrated in Figure 13, the εHOMO and εLUMO energies were calculated using the B3LYP/6–31 G* method within Gaussian software.

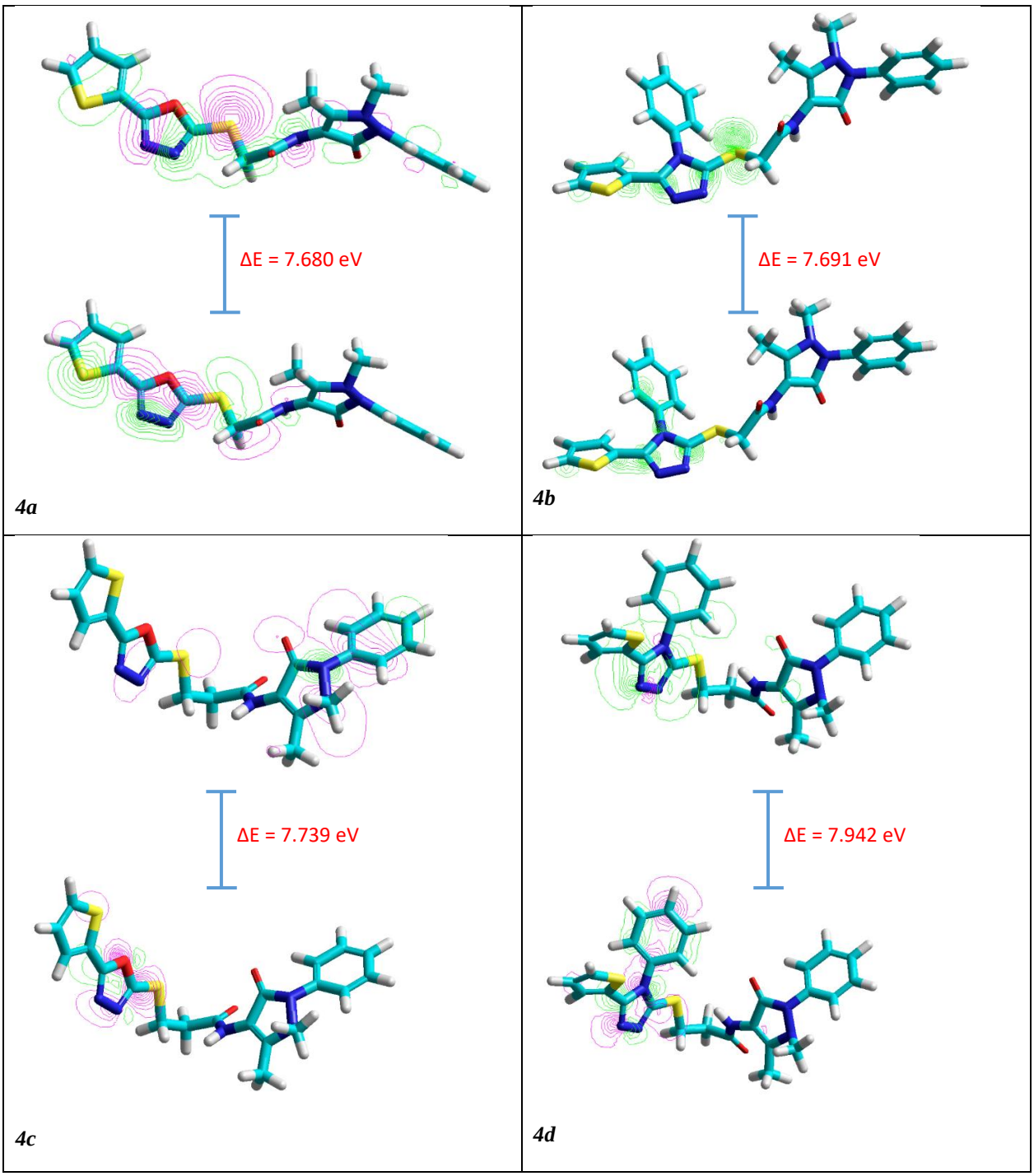

Figure 13. The molecular orbitals of the molecules that are most occupied and lowest vacant.

The equations provided are used to compute various properties of organic compounds, such as additional electronic charge (ΔNmax), global electrophilicity (ΔG), absolute softness (σ), global softness (S), separation energies (ΔE), absolute electronegativities (χ), chemical potentials (Pi), absolute hardness (η), and global electrophilicity (ΔG), and global softness (ΔNmax), as outlined in Equations 2 through 9.

$$\Delta E = \varepsilon_{LUMO} - \varepsilon_{HOMO} \quad (2)$$

$$\chi = -1/2\,(\varepsilon_{LUMO} - \varepsilon_{HOMO}) \quad (3)$$

$$P_i = \chi \quad (4)$$

$$\eta = (\varepsilon_{LUMO} - \varepsilon_{HOMO})/2 \quad (5)$$

$$\omega = \chi^2/2\eta \quad (6)$$

$$\Delta N_{max} = -P_i/\eta \quad (7)$$

$$\sigma = 1/\eta \quad (8)$$

$$S = 1/2\eta \quad (9)$$

Table 4 presents all quantum chemical parameters for the compounds generated utilizing equations 2 through 9.

Table 4. The synthesized compounds' computed quantum chemical parameters

Comp.	εHOMO	εLUMO	ΔE	χ	Pi	η	ω	σ	s	ΔNmax
4a	-8.740	-1.060	7.680	4.900	-4.900	3.840	3.126	0.260	0.130	1.276
4b	-8.559	-0.868	7.691	4.713	-4.713	3.845	2.888	0.260	0.130	1.225
4c	-8.709	-0.970	7.739	4.839	-4.839	3.869	3.026	0.258	0.129	1.250
4d	-8.549	-0.607	7.942	4.578	-4.578	3.971	2.638	0.251	0.125	1.152

According to Table 4, the stability of the produced compounds is indicated by the negativity of both the HOMO and LUMO, as well as their surrounding orbitals, as noted in Tabti et al. (2024) and El Azab et al. (2021). The chemical reactivity, denoted by the energy gap (ΔE), suggests that a lower ΔE value indicates higher reactivity or less stability, as discussed by Łączkowski et al. (2018). The ranking of compounds based on their ΔE values is as follows: 4b (7.691) > 4a (7.680) > 4c (7.739) > 4d (7.942) > 4c, with compound 4d being identified as the most stable. One of the essential quantum chemical descriptors for assessing activity is the electrophilicity index (α), which is crucial in measuring biological activity in drug-receptor interactions. This index evaluates the energy stabilization when the system acquires an additional electrical charge from its surroundings, with higher α values indicating a better capacity for electron acceptance, as highlighted by Jasim et al. (2020). Hence, the compounds with the highest electron-accepting capabilities are 4a (3.126) > 4c (3.026) > 4b (2.888) > 4d (2.638). The parameters η and σ play significant roles in quantifying both molecule stability and reactivity, as discussed by BAĞLAN et al. (2023) and Talmaciu et al. (2016). Compound 4a, with a η value of 3.840 eV, exhibits the lowest chemical hardness (softness) among all compounds studied, suggesting it to be the most reactive. Conversely, compound 4d, with η = 3.971 eV, displays higher stability compared to other compounds. The concepts of Pi and the parameters χ are related, where the global softness σ represents the inverse of the global hardness. Furthermore, compound 4a demonstrates a higher electronegativity value (χ = 4.900 eV) compared to other compounds, positioning it as the most efficient electron acceptor, aligning with its electrophilicity index (α) value.

Conclusion

The findings of the recent study strongly indicate that certain derivatives of 4-aminoantipyrine exhibit significant inhibition of both the active mu-opioid and kappa-opioid receptors, suggesting potential therapeutic applications in analgesic treatment. Molecular docking investigations and density functional theory (DFT) studies support these findings, highlighting the potency of these compounds. Further exploration of these four compounds is warranted for the advancement of novel molecules in drug development.

Disclosure statement

The authors declare no conflict of interest.

Acknowledgement

The author would like to thank Dr. Basim J. Hameed for helping with *in vivo* analgesic evaluation.

References

1. Adithya Krishnan, M., Saranyaparvathi, S., Raksha, C., Vrinda, B., Girish, C. G., Kulkarni, N. V., & Kharisov, B. I. (2022). Transition metal complexes of 4-aminoantipyrine derivatives and their antimicrobial applications. *Russian Journal of Coordination Chemistry*, *48*(11), 696-724.
2. Agu, P. C., Afiukwa, C. A., Orji, O. U., Ezeh, E. M., Ofoke, I. H., Ogbu, C. O., ... & Aja, P. M. (2023). Molecular docking as a tool for the discovery of molecular targets of nutraceuticals in diseases management. *Scientific Reports*, *13*(1), 13398.
3. Alam, M. S., Choi, J. H., & Lee, D. U. (2012). Synthesis of novel Schiff base analogues of 4-amino-1, 5-dimethyl-2-phenylpyrazol-3-one and their evaluation for antioxidant and anti-inflammatory activity. Bioorganic & medicinal chemistry, 20(13), 4103-4108.
4. Alkhzem, A. H., Woodman, T. J., & Blagbrough, I. S. (2022). Design and synthesis of hybrid compounds as novel drugs and medicines. *RSC advances*, *12*(30), 19470-19484.
5. Ascer, E., Bertolami, M. C., Venturinelli, M. L., Buccheri, V., Souza, J., Nicolau, J. C., ... & Serrano Jr, C. V. (2004). Atorvastatin reduces proinflammatory markers in hypercholesterolemic patients. Atherosclerosis, 177(1), 161-166.
6. Asif, M., Imran, M., & Husain, A. (2021). Approaches for chemical synthesis and diverse pharmacological significance of pyrazolone derivatives: a review. *Journal of the Chilean Chemical Society*, *66*(2), 5149-5163.
7. Bachurin, S. O., Makhaeva, G. F., Shevtsova, E. F., Aksinenko, A. Y., Grigoriev, V. V., Shevtsov, P. N., ... & Richardson, R. J. (2021). Conjugation of aminoadamantane and γ-carboline pharmacophores gives rise to unexpected properties of multifunctional ligands. *Molecules*, *26*(18), 5527.
8. BAĞLAN, M., GÖREN, K., & YILDIKO, Ü. (2023). DFT Computations and Molecular Docking Studies of 3-(6-(3-aminophenyl) thiazolo [1, 2, 4] triazol-2-yl)-2H-chromen-2-one (ATTC) Molecule. *Hittite Journal of Science and Engineering*, *10*(1), 11-19.
9. Bilal, M. S., Ejaz, S. A., Zargar, S., Akhtar, N., Wani, T. A., Riaz, N., ... & Umar, H. I. (2022). Computational investigation of 1, 3, 4 oxadiazole derivatives as lead inhibitors of VEGFR 2 in comparison with EGFR: Density functional theory, molecular docking and molecular dynamics simulation studies. *Biomolecules*, *12*(11), 1612.
10. Blanco-Colio, L. M., Tuñón, J., Martín-Ventura, J. L., & Egido, J. (2003). Anti-inflammatory and immunomodulatory effects of statins. *Kidney international*, *63*(1), 12-23.

11. Bulcao, C., Ribeiro-Filho, F. F., Sanudo, A., & Roberta Ferreira, S. G. (2007). Effects of simvastatin and metformin on inflammation and insulin resistance in individuals with mild metabolic syndrome. American journal of cardiovascular drugs, 7, 219-224.
12. Chandrashekar, N. S., & Rani, R. S. (2008). Physicochemical and pharmacokinetic parameters in drug selection and loading for transdermal drug delivery. *Indian journal of pharmaceutical sciences*, *70*(1), 94.
13. El Azab, I. H., El-Sheshtawy, H. S., Bakr, R. B., & Elkanzi, N. A. (2021). New 1, 2, 3-triazole-containing hybrids as antitumor candidates: Design, click reaction synthesis, DFT calculations, and molecular docking study. *Molecules*, *26*(3), 708.
14. Endo, A. (2010). A historical perspective on the discovery of statins. *Proceedings of the Japan Academy, Series B*, *86*(5), 484-493.
15. Ezeja, M. I., Omeh, Y. S., Ezeigbo, I. I., & Ekechukwu, A. (2011). Evaluation of the analgesic activity of the methanolic stem bark extract of Dialium guineense (Wild). *Annals of medical and health sciences research*, *1*(1), 55-62.
16. Fadda, A. A., & Elattar, K. M. (2015). Design and synthesis of some enaminonitrile derivatives of antipyrine as potential novel anti-inflammatory and analgesic agents. Journal of Biosciences and Medicines, 3(11), 114.
17. Ganeshpurkar, A., & Rai, G. (2013). Experimental evaluation of analgesic and anti-inflammatory potential of Oyster mushroom Pleurotus florida. *Indian journal of pharmacology*, *45*(1), 66-70.
18. Glassman, P. M., & Muzykantov, V. R. (2019). Pharmacokinetic and pharmacodynamic properties of drug delivery systems. *Journal of Pharmacology and Experimental Therapeutics*, *370*(3), 570-580.
19. Jasim, E. Q., Dhaif, H. K., MUHAMMAD-ALI, M. A. M. A., & Munther, A. (2020). SYNTHESIS, CHARACTERIZATION, ANTIFUNGAL ACTIVITY AND STRUCTURE--ACTIVITY RELATIONSHIPS: STUDY OF SOME MONO- AND DI-SCHIFF BASES. *Periódico Tchê Química*, *17*(34).
20. Kitas, G. D., Nightingale, P., Armitage, J., Sattar, N., Belch, J. J., Symmons, D. P., ... & Isdale, A. (2019). A multicenter, randomized, placebo-controlled trial of atorvastatin for the primary prevention of cardiovascular events in patients with rheumatoid arthritis. *Arthritis & rheumatology*, *71*(9), 1437-1449.
21. Łączkowski, K. Z., Biernasiuk, A., Baranowska-Łączkowska, A., Zavyalova, O., Redka, M., & Malm, A. (2018). Synthesis, lipophilicity determination, DFT calculation, antifungal and DPPH radical scavenging activities of tetrahydrothiophen-3-one based thiazoles. *Journal of Molecular Structure*, *1171*, 717-725.
22. Meanwell, N. A. (2023). The pyridazine heterocycle in molecular recognition and drug discovery. *Medicinal Chemistry Research*, *32*(9), 1853-1921.
23. Mishra, D., Singh, R., & Rout, C. (2017). A facile amidation of chloroacetyl chloride using DBU. *Int J ChemTech Res*, *10*(3), 365-72.
24. Mohammad, A. E., Muhammad-Ali, M. A., & Jasim, E. Q. (2022). Synthesis, docking study, and biological evaluation of 4-aminoantipyrine-isoniazid derivatives as a hybrid antibacterial and analgesic agents. *Periodico Tche Quimica (Online)*, *42*, 12-27.
25. Mohammad, A. E., Muhammad-Ali, M. A., Hameed, B. J., & Shaheed, D. Q. (2021). Design, synthesis, and characterization of some novel 4-aminoantipyrine derivatives and evaluation of their activity as analgesic agents. *Acta Poloniae Pharmaceutica*, *78*(5), 627-634.
26. Mohan, P., Sharma, A. K., Sinha, S., & Sabarad, R. (2022). An experimental study of rosuvastatin's analgesic effect and its interaction with etoricoxib, tramadol, amlodipine, and amitriptytline in albino mice. medical journal armed forces india, 78, S61-S68.
27. Mohanram, I., & Meshram, J. (2014). Synthesis and biological activities of 4-aminoantipyrine derivatives derived from betti-type reaction. *International Scholarly Research Notices*, *2014*.
28. Murtaza, S., Akhtar, M. S., Kanwal, F., Abbas, A., Ashiq, S., & Shamim, S. (2017). Synthesis and biological evaluation of schiff bases of 4-aminophenazone as an anti-inflammatory, analgesic and antipyretic agent. Journal of Saudi Chemical Society, 21, S359-S372.
29. Proksch, E., Elias, P. M., & Feingold, K. R. (1990). Regulation of 3-hydroxy-3-methylglutaryl-coenzyme A reductase activity in murine epidermis. Modulation of enzyme content and activation state by barrier requirements. The Journal of clinical investigation, 85(3), 874-882.
30. Rusu, A., Moga, I. M., Uncu, L., & Hancu, G. (2023). The Role of Five-Membered Heterocycles in the Molecular Structure of Antibacterial Drugs Used in Therapy. *Pharmaceutics*, *15*(11), 2554.
31. S Antonopoulos, A., Margaritis, M., Lee, R., Channon, K., & Antoniades, C. (2012). Statins as anti-inflammatory agents in atherogenesis: molecular mechanisms and lessons from the recent clinical trials. Current pharmaceutical design, 18(11), 1519-1530.
32. Sahoo, J., Sahoo, C. R., Sarangi, P. K. N., Prusty, S. K., Padhy, R. N., & Paidesetty, S. K. (2020). Molecules with versatile biological activities bearing antipyrinyl nucleus as pharmacophore. *European Journal of Medicinal Chemistry*, *186*, 111911.
33. Shyma, P. C., Kalluraya, B., Peethambar, S. K., Telkar, S., & Arulmoli, T. (2013). Synthesis, characterization and molecular docking studies of some new 1, 3, 4-oxadiazolines bearing 6-methylpyridine moiety for antimicrobial property. *European Journal of Medicinal Chemistry*, *68*, 394-404.
34. Singh, P., Kohr, D., Kaps, M., & Blaes, F. (2009). Influence of statins on MHC class I expression. Annals of the New York Academy of Sciences, 1173(1), 746-751.

35. Sohail, R., Mathew, M., Patel, K. K., Reddy, S. A., Haider, Z., Naria, M., ... & Akbar, A. (2023). Effects of non-steroidal anti-inflammatory drugs (NSAIDs) and gastroprotective NSAIDs on the gastrointestinal tract: a narrative review. *Cureus*, *15*(4).
36. Tabti, K., Sbai, A., Maghat, H., Lakhlifi, T., & Bouachrine, M. (2024). Computational assessment of the reactivity and pharmaceutical potential of novel triazole derivatives: An approach combining DFT calculations, molecular dynamics simulations, and molecular docking. *Arabian Journal of Chemistry*, *17*(1), 105376.
37. Talmaciu, M. M., Bodoki, E., & Oprean, R. (2016). Global chemical reactivity parameters for several chiral beta-blockers from the Density Functional Theory viewpoint. *Clujul medical*, *89*(4), 513.
38. Tüzün, B., & Bhawsar, J. (2021). Quantum chemical study of thiaozole derivatives as corrosion inhibitors based on density functional theory. *Arabian Journal of Chemistry*, *14*(2), 102927.
39. Van de Ree, M. A., Huisman, M. V., Princen, H. M. G., Meinders, A. E., Kluft, C., & DALI-Study Group. (2003). Strong decrease of high sensitivity C-reactive protein with high-dose atorvastatin in patients with type 2 diabetes mellitus. Atherosclerosis, 166(1), 129-135.
40. Wang, Y., Song, H., Szabó, I., Czakó, G., Guo, H., & Yang, M. (2016). Mode-specific SN2 reaction dynamics. *The Journal of Physical Chemistry Letters*, *7*(17), 3322-3327.
41. Yimer, T., Birru, E. M., Adugna, M., Geta, M., & Emiru, Y. K. (2020). Evaluation of analgesic and anti-inflammatory activities of 80% methanol root extract of Echinops kebericho M.(Asteraceae). *Journal of Inflammation Research*, 647-658.
42. Yu, J., Su, N. Q., & Yang, W. (2022). Describing chemical reactivity with frontier molecular orbitalets. *JACS Au*, *2*(6), 1383-1394.